

Enabling the mass production of a chip-scale laser cooling platform

Alan Bregazzi^a, Sean Dyer^a, Paul F. Griffin^a, David P. Burt^b, Aidan S. Arnold^a, Erling Riis^a,
and James P. McGilligan^{a,b}

^aSUPA and Department of Physics, University of Strathclyde, G4 0NG, United Kingdom

^bKelvin Nanotechnology, University of Glasgow, G12 8LS, United Kingdom

ABSTRACT

A low-cost, mass-producible laser-cooling platform would have a transformative effect in the burgeoning field of quantum technologies and the wider research of atomic sensors. Recent advancements in the micro-fabrication of diffractive optics and vacuum apparatus have paved the way for a simple, stackable solution to the laser cooling of alkali atoms. In this paper we will highlight our recent investigations into a chip-scale, cold-atom platform, outlining our approach for on-chip wavelength referencing, examining a solution for imaging atoms in a planar stacked device, and finally discussing the limitations to passively pumped vacuum longevity. These results will be discussed in the context of an outlined road-map for the production and commercialisation of chip-scale, cold-atom sensors.

Keywords: MEMS, cold-atom, atomic-clock, metrology, chip-scale, micro-fabrication, wavelength-reference

1. INTRODUCTION

The realisation of laser cooling has enabled a revolution in the capabilities of precision metrology.¹⁻³ The significantly reduced velocity distribution of cold atom samples enables trapping and probing of atoms with long interrogation times and narrow frequency features. As well as being a critical tool in timing, laser cooled atoms provide increased performance in interferometry for measurements of acceleration, rotation and gravimetry.⁴ It is the increased stability and precision found in cold atoms that place them at the forefront of current endeavours in quantum computers and quantum simulations.^{5,6}

A common work-horse that is used as the primary step in cooling atoms below milli-Kelvin temperatures is the magneto-optical trap (MOT).⁷⁻⁹ In the MOT, red-detuned laser light is used to impart momentum kicks on the atoms by optical pumping through cycling transitions, taking momentum from the interacting atoms in the process. A gradient magnetic field is required to provide a spatially varying scattering force through the Zeeman effect. Laser cooling is typically carried out with 6 laser beams in a retro-reflected configuration to satisfy 3 dimensional cooling, which ultimately requires a sizeable optical footprint. Furthermore, the atomic source being laser cooled requires a clean vacuum environment, with total background pressures typically below 10^{-7} mbar to reduce thermal collisions that would hinder the cooling process. The vacuum environment is commonly provided in a stainless-steel chamber, with sufficient optical access, mechanically pumped-down to ultra-high-vacuum (UHV) pressures. The UHV pressures of the chamber is subsequently maintained by active pumping with an ion pump. Overall, these critical components at the core of laser cooling require a significant size, weight, and power (SWaP) consumption to provide a suitable environment for cold-atom metrology.

This paper will look at the recent advancements that have been made to miniaturise laser cooling at the University of Strathclyde and within the wider atomic physics community, with a specific focus on micro-fabricated components that facilitate the mass production of cold-atom platforms. Additionally, the outlined vision for chip-scale atomic sensors will highlight current research that has the capability to provide a step-change in quantum technology.

Further author information: (Send correspondence to J.P.M)
E-mail: james.mcgilligan@strath.ac.uk

2. A MASS PRODUCIBLE COLD-ATOM PLATFORM

In this section we outline our vision for a fully chip-scale, cold-atom system constructed around components that can be micro-fabricated for mass production and reproducibility at a low cost. The vision of a fully integrated system, shown in Figure. 1, is presented as a 4-inch diameter wafer stack. The wafer stack is anodically bonded in a glass-silicon-glass sandwich. This method of forming a hermetic seal between the glass-silicon interface has been well established in micro-electro-mechanical-systems (MEMS),¹⁰ pioneering the advancement of miniature vapour cells for clocks,^{11,12} magnetometers¹³ and wavelength references.^{14,15} In our presented road-map, a 5 mm thick silicon wafer has two independently-etched cavities for atomic spectroscopy and laser cooling, highlighted in inset (i) and (ii) respectively.

In previous literature, MEMS vapour cells have typically been formed from silicon anodically bonded to borosilicate glass (BSG) due to its large ion content enabling bonding at $\sim 300^\circ\text{C}$, as well as possessing a coefficient of thermal expansion that is well matched to silicon.^{16,17} Recent work has shown that compatibility of aluminosilicate glass (ASG) for MEMS vapour cells, while exhibiting a significantly reduced helium permeation rate compared to borosilicates.¹⁸ Although ASG is not an essential component for thermal atom vapour cells, the reduced helium permeation provides an improved pressure longevity for passively pumped cold atom cells,^{19,20} that would otherwise be rapidly degraded by the permeation of atmospheric helium. Additionally, ASG has been demonstrated to produce a hermetic anodic bond with silicon at temperatures as low as 150°C when doped with a larger alkali ion content,²¹ expanding the compatibility of MEMS cell technology with integrated components that cannot sustain a high bonding temperature.

Prior to cell closure, an alkali source must be added to each cell by a deposition method that is compatible with mass production. As such, we discuss simple, mass producible methods for clean alkali deposition in MEMS UHV cells in Section 5. After wafer bonding, a copper pinch off tube is adhered to a hole drilled in the upper glass of the laser cooling cell. This enables the cell to be pumped-down to UHV by a larger pumping apparatus,

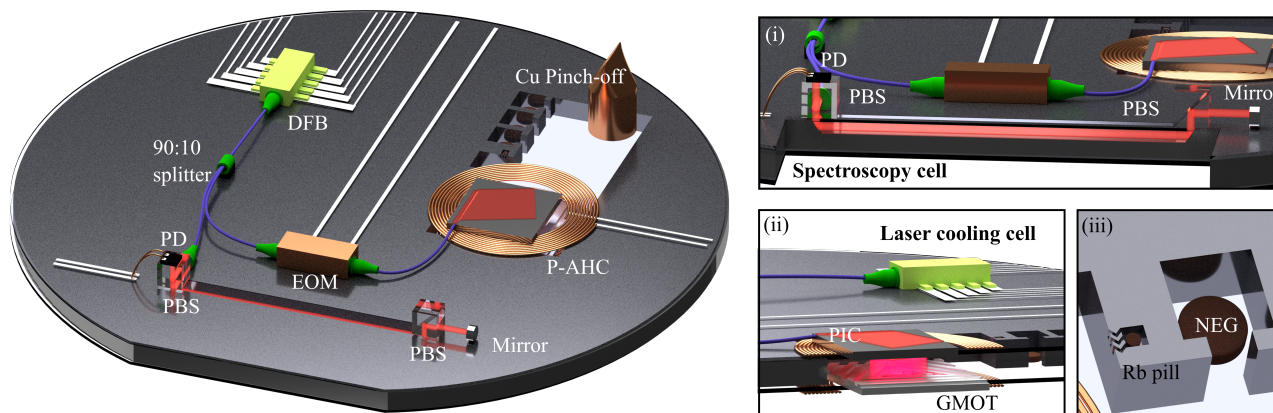


Figure 1. An illustration of a micro-fabricated laser cooling platform on a 4-inch diameter, 6 mm thick wafer stack. The stack is composed of an aluminosilicate glass (ASG)-Si-ASG sandwich. A distributed-feedback (DFB) laser is surface mounted and locally temperature stabilised. The output light is coupled into a 90:10 fibre splitter for cooling and spectroscopy respectively. The output of the spectroscopy fibre is collimated and aligned into a polarising-beam-splitter (PBS). The PBS reflects the light into an elongated, wet-etched spectroscopy cell for wavelength referencing. The output of the cell couples through a second PBS and is retro-reflected from a surface bonded mirror. The cooling fibre arm is modulated through an electro-optical-modulator (EOM) with fibre in and out. In this illustrated roadmap we visualise the output of the cooling fibre being coupled through a slab-mode photonic chip, although this technology requires further development time. The output of the chip is aligned onto a micro-fabricated grating chip, housed inside a pre-evacuated ultra-high vacuum cell. The cell has been pumped-down through a copper pinch-off tube, which is then cold-welded shut to isolate the cell. Planar-aligned anti-Helmholtz coils are deposited on the glass surfaces to provide a sufficient gradient magnetic field for laser cooling. Inset (i): Cut-away illustration of the wet-etched, elongated spectroscopy cell for laser locking. Inset (ii): Cut-away illustration of the UHV cell, etched into the silicon wafer and pre-evacuated to suitable vacuum pressures for laser cooling. Inset (iii): Close-up of the alkali pill and non-evaporable-getter (NEG) chambers used within both the spectroscopy and laser cooling cells to control the vacuum and alkali environment.

then sealed by a cold-weld for vacuum isolation.

Following the formation of the wafer stack, optical components can be adhered to the upper glass surface. In our presented vision, a single distributed-feedback (DFB) laser is adhered to the upper glass surface, with aluminium deposited on the surface below for localised temperature stabilisation of the laser. Recent work has demonstrated chip-scale DFB lasers with line-widths and output powers compatible with laser cooling of rubidium.²² The decreased thermal conductivity of the surrounding glass wafer enables a fast time constant for thermal feedback through the locally deposited aluminium below the laser body. The wavelength of the DFB is centred around 780.24 nm to address the cooling transition of D₂ ⁸⁷Rb. Additionally, the current is modulated at ~6.5 GHz to provide 5 % sidebands for the re-pumping transition. The fibre output of the DFB is connected to a fibre splitter and divided into two arms, with a 90:10 ratio, for laser cooling and wavelength referencing respectively. An optical isolator (OI) may be added at the output of the DFB fibre to reduce etaloning effects from reflective optics further down the path. One arm of the fibre splitter is collimated and aligned through a half-waveplate and a surface-adhered polarising-beam-splitter (PBS). The reflected light from the PBS is coupled into an elongated vapour cell, discussed in Section 3. The cell contains rubidium vapour to enable laser frequency stabilisation with saturated absorption spectroscopy.

The second arm of the fibre splitter can be connected to a phase electro-optical modulator (EOM) to provide side-bands at 6.8 GHz, with an equal amplitude to the carrier frequency, for future clock measurements with coherent population trapping (CPT) on the Rb D₂ line.^{23,24} Ideally, the light is then coupled into an apodised grating within a photonically integrated circuit (PIC).²⁵ Such chips have demonstrated the ability to couple light out of a waveguide and into free-space in a collimated, Gaussian mode with a ~3 mm beam waist.²⁶ While the cell and grating chip technology outlined in this road-map are built around existing technology, the PIC has not yet reached a technology readiness level that could output a beam width compatible with laser cooling in a GMOT. The progress of this research to date is outlined in Section 4.

The collimated light propagates through the laser cooling cell, etched into the silicon surface. However, this cell has been pre-evacuated and pumped down to ultra-high-vacuum (UHV) through the pinched-off copper tube adhered to the upper glass surface. An alkali atom background density is provided from an externally activated micro-pill dispenser, with the UHV pressure being maintained through passive pumping by non-evaporable-getters (NEGs). The laser light is incident upon a micro-fabricated grating chip, which provides the additionally required laser beams for 3 dimensional cooling by diffracting the incident light at angles relative to the period of the gratings etched into the chip surface.²⁷ The technical aspects of the laser cooling components are discussed in Section 4.

3. LASER LOCKING AND FREQUENCY CONTROL

Devices relying on an atomic wavelength reference are widely implemented in the measurement of magnetic fields,²⁸ time,²⁹ rotation³⁰ and length,¹⁴ finding application in navigation, geological surveying, medicine, communication and finance. Well defined atomic transitions can be extracted from atomic vapour using techniques such as saturated absorption spectroscopy. The alkali source under interrogation is typically contained within a 10 cm long glass-blown cell, to provide sufficient absorption of resonant light within the alkali vapour, as given by Beer-Lambert law $I(x) = I_0 \exp(-\alpha x)$, where $I(x)$ is the intensity of the light at position x , I_0 is the incident beam intensity, and α is the absorption coefficient; dependent on the frequency of the incident light and the temperature of the atomic medium. Saturated absorption spectroscopy in such glass-blown vapour cells has demonstrated a frequency stability of $3 \times 10^{-12} \tau^{-1/2}$,^{31,32} where the short-term limitation was attributed to the frequency modulation of the laser diode for locking electronics.

In the past decade, significant effort has been made to miniaturise atomic wavelength references through the development of micro-fabricated alkali vapour cells.¹⁰ The realisation of miniature vapour cells has paved the way for chip-scale atomic clocks and commercial atomic products.¹¹ However, these miniaturised packages are typically limited in performance by a poor signal-to-noise ratio resulting from the short absorption path length in straight lined, ~2 mm thick silicon cells,¹⁷ resulting from technical difficulties and etch times for dry and wet etch processes respectively. The theoretically expected absorption for different cell path lengths are highlighted in Fig. 2 (a), with an illustration of the cell geometry and optical path length in (b)-(d). For each of the simulated absorption spectra the cell temperature was set at 20°C. The absorption of the 10 cm glass-blown cell, shown in black, reaches a maximum absorption of 50%, whilst the 2 mm MEMS cell is less than 5% under the same

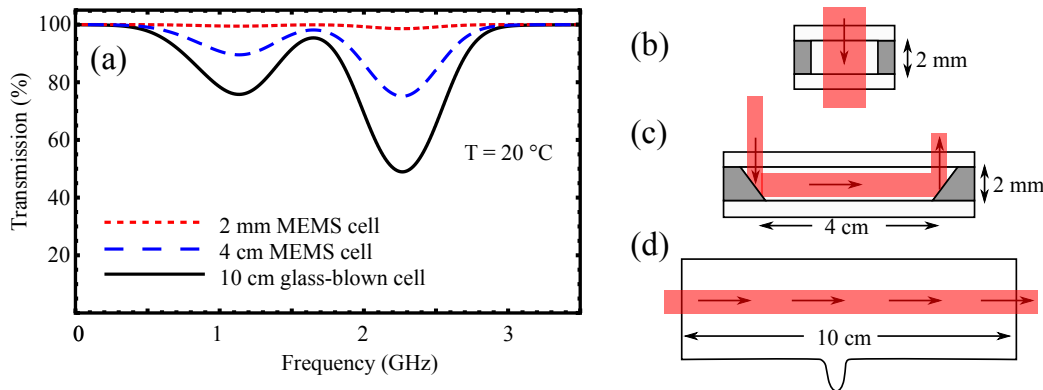


Figure 2. (a): Theoretical Doppler absorption at 20°C for cells with an optical path length of 2 mm, 4 cm, and 10 cm for a single pass MEMS cell, elongated light routed MEMS cell, and standard glass-blown cell respectively. (b)-(d): Illustration of optical interrogation and path length from cell geometries.

conditions. However, a more comparable absorption to the glass-blown cell can be achieved in the 2 mm MEMS cell when heated to 60°C. Although some performance gains can be reclaimed by increasing the vapour density via external heating of the cell, the heating apparatus requires additional circuitry, heaters and electrical power consumption, degrading the SWaP footprint of the device. Recent literature has overcome the performance of standard sub-Doppler spectroscopy of alkali atoms by demonstrating an optical wavelength reference in a Rb MEMS cell using two-photon spectroscopy to demonstrate an instability of $1.8 \times 10^{-13} \tau^{-1/2}$.³³ Alternative geometries have also been explored to increase the path length, such as taking advantage of the anisotropic wet etch of the {111} crystallographic plane at 54.7° in an elongated cell.¹⁵ However, since incident orthogonal light will not be routed through the long axis of the cell at this angle, a diffraction grating is etched into the upper glass wafer, providing a significant over complication in fabrication, cost, wafer alignment and yield.

A simplified scenario that we are currently pursuing in our chip-scale cooling apparatus will use angled walls to route light through the long axis of the vapour cell without the need for additional complexity such as the diffractive optical element used in Ref.¹⁵ Our proposed scheme will use angled silicon walls, coated in evaporated Al reflectors, to route light through a 4 cm long vapour cell. The end of the cell will incorporate a reflective surface to retro-reflect the light back along the incident beam to enable saturated absorption spectroscopy for laser locking, as shown in Fig. 2 (c). The expected absorption for this cell is shown in Fig. 2 (a) in blue, demonstrating a significant improvement on the standard 2 mm thick MEMS cell geometry without the need for additional cell heating.

An additional novelty that we will investigate in the spectroscopy cell is the ability to offset lock the laser in real time with an external magnetic field to perturb the atomic resonance frequency. The reproducible control of the laser frequency lock point in real time could potentially be used for frequency ramps required in optical molasses within the cold atom cell, in turn mitigating the need for additional optical components further down the manufacturing line.

4. OPTICAL COMPONENTS FOR LASER COOLING

In recent years, significant effort has been placed on the miniaturisation of laser cooling optics to facilitate sensors being brought out of the laboratory environment and into society where they will have the largest economic and technological impact. A primary advancement to the miniaturisation of optical components in laser cooling is the pyramid MOT.³⁴ The pyramid MOT takes a single incident beam, with a beam waist that fills the surface of a conical structured mirror, where the reflected light provide the required additional orders for 3-dimensional laser cooling. However, since the cold atom sample would form inside the pyramidal structure, optical access is difficult for imaging and probing the cold sample. To overcome this, the angle of the mirrors can be reduced to a tetrahedral configuration, where the optical overlap region is then out and above the mirrored structure for clear optical access.³⁵ A more recent advancement that follows this route is the grating magneto-optical-trap

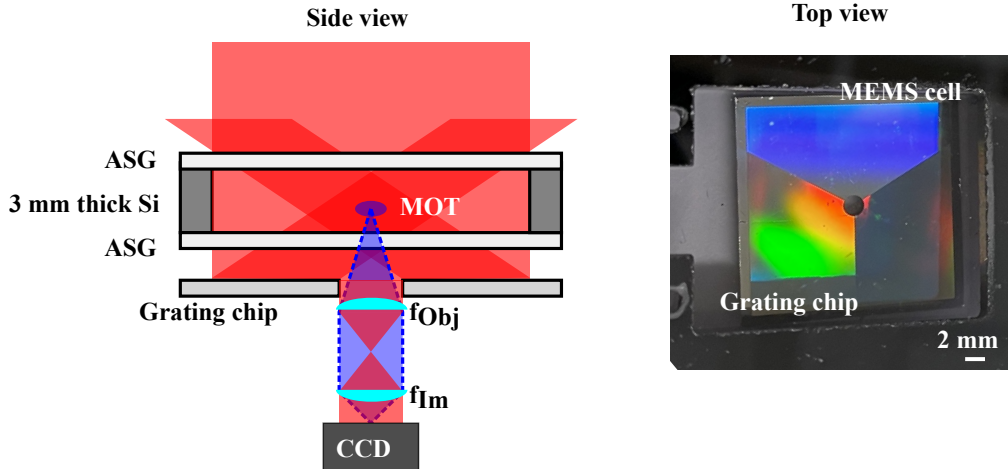


Figure 3. Cooling and imaging schematic used for the MEMS-GMOT platform. The side view illustrates the wafer stack, composed of a 3 mm thick silicon wafer sandwiched between two aluminosilicate (ASG) glass wafers. The single incident beam is aligned onto the grating chip, below the glass window, with a hole cut at the centre for absorption imaging. The stackable imaging system collimates the MOT fluorescence with f_{Obj} placed immediately below the grating hole. The MOT signal is then focused onto the CCD, while the laser light is collimated at this point. This lens configuration could be replaced with micro-fabricated Fresnel lens, etched into the glass wafer. The top view shows a 20 mm diameter grating chip, with a 2 mm cut central hole for imaging. The MEMS cell is fabricated to have a wide enough vacuum region to house the full grating chip surface.

(GMOT).³⁶ Similar to the pyramidal MOT, the GMOT reduces the 6 laser beams used for 3-dimensional laser cooling down to a single incident beam. However, rather than using the reflected orders from a mirror surface, the GMOT uses the diffracted orders from a grating chip, where the incident light is diffracted at an angle relative to the grating period. This is advantageous to minimising the footprint of laser cooling, as the required optical component is now planar. The scalability of the GMOT has been emphasized further by the micro-fabricated GMOT chips, etched into silicon substrates and coated in reflective metals, capable of trapping 10^6 atoms at $3 \mu\text{K}$,^{27,37} with atom numbers as large as $\sim 10^8$ having been previously shown.³⁸ This technology is now a commercially available product.³⁹

Previous work has shown the compatibility of micro-fabricated GMOT chips with MEMS UHV cells for laser cooling of ^{85}Rb .⁴⁰ However, the miniaturised components have a restricted optical access, such that atom number extraction is non-trivial due to the remaining imaging angles being dominated by surface scatter from the grating and cell surface. In previous work, imaging of the MEMS GMOT was achieved using a two-photon process to drive atoms through a cascade at 420 nm. The addition of a narrow band-pass filter at 420 nm to the imaging optics ensures that only atomic fluorescence is captured during imaging, resulting in background-free images of the cold atom sample. However, although the cold atom sample can be resolved in this apparatus, direct evaluation of the trapped atom number is frustrated by the non-trivial optical pumping scheme.

Our recent research has looked to enable a simple method for atom number extraction in this stacked apparatus by laser cutting a hole in the grating chip centre. Once a cold-atom sample is loaded in the cell, the single incident cooling beam intensity is dropped to enable absorption imaging through an objective lens placed immediately behind the grating hole. An illustration and top down view of the platform is shown in Fig. 3. The light is then imaged onto a CCD, permitting quantitative analysis of the MEMS-GMOT dynamic range and enabling further investigations into system optimisation.⁴¹ This simple imaging method has been used to resolve a MEMS-GMOT atom number of $\approx 5 \times 10^5$ atoms. The amalgamation of these micro-fabricated components forms an ideal potential platform for future chip-scale atomic sensors. However, methods for coupling the incident laser light in a compact manner remain ambiguous.

Solving a chip-scale method for the generation, shape and direction of the incident light has recently been investigated with planar optics.⁴² The light source is first injected into a nano-photonics waveguide within a photonic integrated circuit (PIC), that is etched into a SiN substrate. This technology has been previously demonstrated with MEMS vapour cells in Ref.¹⁴ The PIC routes light through a SiN slab-mode and into an

apodised diffraction grating, which couples the light into free-space with a collimated Gaussian mode. Although the output beam was collimated with a $1/e^2$ waist of $140\ \mu\text{m}$ and 4° angle with respect to the chip surface, further investigations have looked at large area grating couplers that would be well suited to stackable cold atom sensors.²⁶ To circumvent the small beam waist, the authors of Ref. [42] employ a metasurface lens, which expands the beam profile while converting the Gaussian shape to a flat-top. The flat top beam is then expanded to fill the surface of a GMOT chip for laser cooling. However, a divergence angle of 7.6° from the metasurface requires a long expansion distance for the incident beam to fill the surface of a 2 cm wide grating chip. Our current investigations have explored the capability of the GMOT to handle diverging beams from standard refractive optics, with a similar divergence angle and distance to Ref.⁴² producing a GMOT. However, significantly wider angles of incident divergent beams may be achievable for laser cooling with a grating chip if novel grating geometries are employed, such as a chirped grating period combined with a binary-blaze profile ramp. Such novel grating chips would facilitate a wider range of potential light coupling methods that would better meet the needs of a chip-scale cold-atom apparatus.

5. VACUUM LONGEVITY FOR COLD ATOM CELLS

To aid the longevity of the UHV MEMS cell, whilst remaining compatible with mass production, a simple solution must be provided for alkali deposition and passive pumping. The first of these topics to be discussed are the methods of providing a clean alkali vapour density within the cell.

The alkali vapour content in cold-atom experiments is typically provided by an ampoule source or resistively heated alkali-metal dispensers (AMDs).^{27,43} However, the need for electrical feedthroughs to activate AMDs, as well as the difficulty of handling alkali ampoules in air, make these unattractive options for chip-scale production. Existing literature has shown the compatibility of azide and chloride compounds with MEMS cells due to their dispensing simplicity during cell fabrication.^{10,44} However, the disassociation of alkali azide produces an abundance of N_2 buffer gas. Although this may prove favourable for vapour cell clocks and magnetometers, the presence of buffer gas would be detrimental in a cold-atom system.

A simple approach to atomic sourcing is the commercially available solid alkali pill, capable of in-air handling and external activation with no significant byproduct atomic species produced.⁴⁵ The reduced complexity of incorporating the pill into the pre-bonded cell, as well as the ability to avoid electrical feedthroughs, make this approach a promising candidate for future chip-scale sensors. The activation routes available for alkali pill dispensers are highlighted in Fig. 4 (a)-(c). The first option shown is the activation of the Rb pill prior to cell closure. The pill is placed inside the pre-bonded Si-ASG cavity and laser heated. During activation the cell is kept at a lower temperature than the surrounding vacuum to enable Rb condensation within the cell, whilst the non-Rb contaminants (N_2 and CO) are pumped away by the larger vacuum. The upper glass is then brought into contact with the Si wafer and anodically bonded. This bonding method is known to release an unspecified amount of O_2 from the edges of the bonding interface, where free oxygen atoms do not join with the Si substrate.^{20,46} This unwanted oxygen content will rapidly deplete the neutral Rb vapour density by forming Rb_2O . It is worth noting that this method has the additional risk of contaminating the bonding surface during the pill activation, which can potentially impact the yield and hermeticity of the cell. To avoid surface contamination, the pill can instead be activated post-bonding, as shown in Fig. 4 (b). However, in this scenario there is no route to remove the non-Rb elements released during pill activation, which will ultimately limit the vacuum pressure and device stability. A simple route to overcome these issues, shown in Fig. 4 (c), is the addition of a NEG pill to sorb the unwanted contaminants from pill activation and the oxygen released during bonding. This enables post-bonding activation while providing a simple route to alkali deposition on the wafer-scale. Due to this simplicity, alkali sourcing from solid state pills is now widespread in vapour cell fabrication,^{14,29,47,48} with recent industrial transfer of vapour cell technology that incorporate an alkali pill source.⁴⁹

Alternative atomic sources exist in the form of recently demonstrated graphite reservoirs. Highly-oriented-pyrolytic-graphite (HOPG) is an attractive candidate from atomic sourcing due to its selective intercalation of alkali atoms, enabling the diffusion of Rb into the bulk of the graphite when heated. Such atomic sources have been demonstrated recently as viable atomic sources for laser cooling apparatus after loading the HOPG from a liquid ampoule source.⁵⁰

An exciting development in graphite based alkali sourcing is the alkali-ion battery (AIB). The AIB utilises

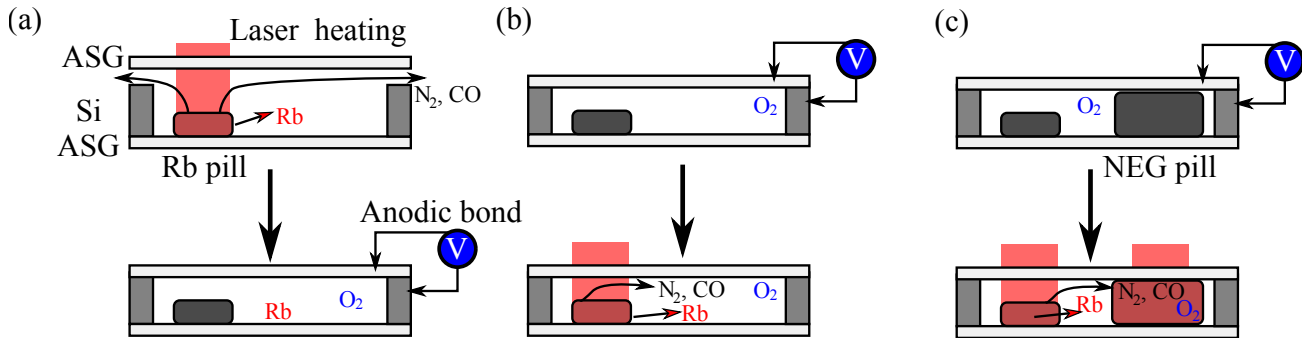


Figure 4. Rubidium cell deposition options. (a): Pill is laser heated before the cell is hermetically sealed. Temperature gradients between the external vacuum and MEMS cell walls can then be used to evacuate the non-Rb contaminants (N₂, CO in this example) while condensing the metal Rb within the cell. Anodic bonding then seals the cell closed with a Rb vapour density. The anodic bonding process provides an additional O₂ contaminant into the cell. (b): The cell is anodically bonded for a hermetic seal prior to pill activation. Once sealed, the pill is laser heated, releasing both the Rb and non-Rb elements into the vapour. (c): A NEG and pill combination are deposited into the cell prior to cell sealing. Both the pill and NEG are laser heated, such that the non-Rb and O₂, produced during the bonding process, diffuse into the NEG bulk and form stable chemical compounds that are irreversible to diffuse back out of the bulk. This leaves a pure Rb vapour density behind in the cell.

electrode plated electrolyte connected to a graphitic reservoir as a voltage controllable source of neutral alkali atoms.⁵¹ The reversible electrochemical disassociation/recombination at the electrode-electrolyte interface enables sourcing and sinking of the alkali content from the reservoir and vacuum environment, permitting a micro-fabricated solution to alkali recycling and density regulation. Recent work has demonstrated the sourcing of a MOT directly from an AIB source,⁵² with sourcing and sinking time constants on the order of 1 s.⁵³ When coupled to a small vacuum system, such as that proposed, the AIB could both potentially extend the vacuum lifetime by providing a clean alkali source and enable a wider field of deployment by regulating the density against environmental temperature fluctuations. However, due to the requirement of electrical feedthroughs for the voltage control of the electrochemical reaction, this device is currently unfavourable for a simple, anodically bonded wafer stack. As such, we propose the best current candidate for atomic sourcing in a mass producible, chip-scale cooling platform as the solid alkali pill, where the silicon frame can be etched to house the pill for external activation from laser heating. An example of the pill chamber is shown in Figure 1, inset (iii), where zig-zag channels provide a fluid connection to the main cell without a direct line of sight to reduce any contaminant spray during activation. The second consideration for vacuum environmental control in the MEMS cell is vacuum pumping. In the absence of active vacuum pumping, the internal cell pressure is rapidly degraded by permeation, material out-gassing and adsorption of contaminants from vacuum surfaces. Typically, a cold-atom vacuum system is maintained by an ion-pump, accelerating electrons between a cathode-anode potential in a magnetic field to ionise and getter elements within the vacuum. However, an applied voltage on the order of a kV is typically required, as well as there being a substantial gradient magnetic field, which is unfavorable in the presence of any atomic spectroscopy. As such, the complexity and vacuum volume associated with ion pumps make these an unattractive candidate for chip-scale devices.

Alternatively, passive pumping materials such as NEG have recently been demonstrated as being capable of extending the vacuum lifetime of cold-atom systems.¹⁹ The commercially available NEG pills contain a getter reducing agent, composed of 84% Zr and 16% Al. The getter material is capable of chemically sorbing vacuum pollutants from the vacuum environment into the bulk of the pill. Once vacuum impurities, such as N₂, CO, and O₂ diffuse into the NEG pill they undergo irreversible chemical reactions that lock them inside the getter material.⁵⁴ Although H₂ will also sorb into the NEG bulk, the H₂ does not form a stable chemical compound that would effectively lock it within the getter bulk. Instead, the diffusion of H₂ into the bulk of the pill can be reversed by further heating of the NEG.⁵⁴

Recent literature has shown that when a single NEG pill was laser activated in a MEMS UHV cell, an order of magnitude improvement was observed on the detection time of the cold-atom sample.¹⁹ However, the NEG materials are not capable of pumping noble gases, such as helium, placing the necessity on helium-impermeable

materials for the cell fabrication.

Due to the attractive properties of NEG, they have been placed at the centre of recent ventures in compact cold atom apparatus.^{55,56} The results in Ref.⁵⁵ use a large pumping-rate, electrically-activated NEG within a machined titanium chamber, of volume 320 cm³, to demonstrate a detection time of the cold-atom sample exceeding 200 days when purely passively pumped. Although this is a very promising result for NEG performance, the electrical feedthroughs are unfavourable for a chip-scale apparatus, such that the NEG pill option is preferred. Additionally the machining of the Ti vacuum body, and attachment of commercial vacuum windows restricts the scalability of this vacuum apparatus to the chip-scale. However, the robust nature of the vacuum, and large atom number, make this platform an ideal base for portable and compact quantum sensors.⁵⁷

A second approach to miniaturised, passively pumped vacuum apparatus is the centilitre-scale, ceramic chamber discussed in Ref.⁵⁶ With easy optical access and a mass producible vacuum body, the 40 cm² ceramic chamber has shown a UHV pressure longevity on the order of a year with a single NEG. Although measurements of the cold atoms were not taken during this window, the demonstration of the vacuum pressure longevity over this time period remains a promising insight to the capabilities of NEG compounds in low-He permeable chambers.

A final notable candidate for future compact, passively pumped vacuum chambers are discussed in Ref.⁵⁸ Here, the authors demonstrate a simple method of 3D printing custom vacuum chambers that are capable of attaining UHV pressures for laser cooling. Currently the scalability of these chambers is limited by the necessity of standard CF window ports. However, it is conceivable that this could be mitigated to further reduce the footprint of the custom chamber designs. With a weight of just 0.25 kg and no significant out-gassing measured,⁵⁹ this platform remains an attractive future candidate for compact sensors, compatible with passive pumping.

Whilst significant miniaturisation has been achieved in the highlighted apparatus, the MEMS GMOT coupled system remains a favourable candidate to facilitate a mass-producible, chip-scale cold atom platform with a significantly reduced volume (2.4 cm³) and weight (~0.1 kg), while maintaining a competitive atom number.

6. CONCLUSION

In conclusion, we have highlighted our road-map for the mass-production of a chip-scale, cold-atom platform. The novel wavelength reference being developed at the University of Strathclyde provides an attractive approach to on-chip frequency stabilisation, with the potential for real-time offset control studies in the near-future. Additionally, we have recently shown that the coupling of the MEMS UHV cell and GMOT chip can trap 5×10^5 atoms, as measured with absorption imaging through a hole cut at the grating centre. The capabilities of passive pumping with NEG materials in this apparatus will be investigated further, with an outlook of systematic improvements to aid the vacuum longevity.

ACKNOWLEDGMENTS

The authors acknowledge funding from Defence Security and Technology Laboratory (DSTL), Engineering and Physical Sciences Research Council (EP/T001046/1), and Defence and Security Accelerator (DASA). A. Bregazzi is funded by a DSTL studentship. J.P.M is funded by a Royal Academy of Engineering Research Fellowship.

REFERENCES

- [1] Heavner, T. P., Jefferts, S. R., Donley, E. A., Shirley, J. H., and Parker, T. E., “NIST-f1: recent improvements and accuracy evaluations,” *Metrologia* **42**, 411–422 (sep 2005).
- [2] Katori, H., “Optical lattice clocks and quantum metrology,” *Nature Photonics* **5**(4), 203–210 (2011).
- [3] Schioppo, M., Brown, R. C., McGrew, W. F., Hinkley, N., Fasano, R. J., Beloy, K., Yoon, T. H., Milani, G., Nicolodi, D., Sherman, J. A., Phillips, N. B., Oates, C. W., and Ludlow, A. D., “Ultrastable optical clock with two cold-atom ensembles,” *Nature Photonics* **11**(1), 48–52 (2017).
- [4] Geiger, R., Landragin, A., Merlet, S., and Pereira Dos Santos, F., “High-accuracy inertial measurements with cold-atom sensors,” *AVS Quantum Science* **2**(2), 024702 (2020).
- [5] Picken, C. J., Legaie, R., McDonnell, K., and Pritchard, J. D., “Entanglement of neutral-atom qubits with long ground-rydberg coherence times,” *Quantum Science and Technology* **4**, 015011 (dec 2018).

- [6] Peaudecerf, B., Andia, M., Brown, M., Haller, E., and Kuhr, S., “Microwave preparation of two-dimensional fermionic spin mixtures,” *New Journal of Physics* **21**, 013020 (jan 2019).
- [7] Weiss, D. S., Riis, E., Shevy, Y., Ungar, P. J., and Chu, S., “Optical molasses and multilevel atoms: experiment,” *J. Opt. Soc. Am. B* **6**, 2072–2083 (Nov 1989).
- [8] Raab, E. L., Prentiss, M., Cable, A., Chu, S., and Pritchard, D. E., “Trapping of neutral sodium atoms with radiation pressure,” *Phys. Rev. Lett.* **59**, 2631–2634 (Dec 1987).
- [9] Monroe, C., Swann, W., Robinson, H., and Wieman, C., “Very cold trapped atoms in a vapor cell,” *Phys. Rev. Lett.* **65**, 1571–1574 (Sep 1990).
- [10] Liew, L.-A., Knappe, S., Moreland, J., Robinson, H., Hollberg, L., and Kitching, J., “Microfabricated alkali atom vapor cells,” *Applied Physics Letters* **84**(14), 2694–2696 (2004).
- [11] Knappe, S., Shah, V., Schwindt, P. D. D., Hollberg, L., Kitching, J., Liew, L.-A., and Moreland, J., “A microfabricated atomic clock,” *Applied Physics Letters* **85**(9), 1460–1462 (2004).
- [12] Hasegawa, M., Chutani, R., Gorecki, C., Boudot, R., Dziuban, P., Giordano, V., Clatot, S., and Mauri, L., “Microfabrication of cesium vapor cells with buffer gas for mems atomic clocks,” *Sensors and Actuators A: Physical* **167**(2), 594–601 (2011). Solid-State Sensors, Actuators and Microsystems Workshop.
- [13] Shah, V., Knappe, S., Schwindt, P. D. D., and Kitching, J., “Subpicotesla atomic magnetometry with a microfabricated vapour cell,” *Nature Photonics* **1**(11), 649–652 (2007).
- [14] Hummon, M. T., Kang, S., Bopp, D. G., Li, Q., Westly, D. A., Kim, S., Fredrick, C., Diddams, S. A., Srinivasan, K., Aksyuk, V., and Kitching, J. E., “Photonic chip for laser stabilization to an atomic vapor with 10^{11} instability,” *Optica* **5**, 443–449 (Apr 2018).
- [15] Chutani, R., Maurice, V., Passilly, N., Gorecki, C., Boudot, R., Abdel Hafiz, M., Abbé, P., Galliou, S., Rauch, J.-Y., and de Clercq, E., “Laser light routing in an elongated micromachined vapor cell with diffraction gratings for atomic clock applications,” *Scientific Reports* **5**(1), 14001 (2015).
- [16] Maurice, V., Rutkowski, J., Kroemer, E., Bargiel, S., Passilly, N., Boudot, R., Gorecki, C., Mauri, L., and Moraja, M., “Microfabricated vapor cells filled with a cesium dispensing paste for miniature atomic clocks,” *Applied Physics Letters* **110**(16), 164103 (2017).
- [17] Kitching, J., “Chip-scale atomic devices,” *Applied Physics Reviews* **5**, 031302 (Sept. 2018).
- [18] Dellis, A. T., Shah, V., Donley, E. A., Knappe, S., and Kitching, J., “Low helium permeation cells for atomic microsystems technology,” *Optics Letters* **41**, 2775 (June 2016).
- [19] Boudot, R., McGilligan, J. P., Moore, K. R., Maurice, V., Martinez, G. D., Hansen, A., de Clercq, E., and Kitching, J., “Enhanced observation time of magneto-optical traps using micro-machined non-evaporable getter pumps,” *Scientific Reports* **10**, 16590 (Oct. 2020).
- [20] Rushton, J. A., Aldous, M., and Himsforth, M. D., “Contributed review: The feasibility of a fully miniaturized magneto-optical trap for portable ultracold quantum technology,” *Review of Scientific Instruments* **85**, 121501 (Dec. 2014).
- [21] Shoji, S., Kikuchi, H., and Torigoe, H., “Low-temperature anodic bonding using lithium aluminosilicate- $\hat{\text{I}}^2$ -quartz glass ceramic,” *Sensors and Actuators A: Physical* **64**(1), 95–100 (1998). Tenth IEEE International Workshop on Micro Electro Mechanical Systems.
- [22] Gaetano, E. D., Watson, S., McBrearty, E., Sorel, M., and Paul, D. J., “Sub-megahertz linewidth 780.24 nm distributed feedback laser for ^{87}Rb applications,” *Opt. Lett.* **45**, 3529–3532 (Jul 2020).
- [23] Elvin, R., Hoth, G. W., Wright, M., Lewis, B., McGilligan, J. P., Arnold, A. S., Griffin, P. F., and Riis, E., “Cold-atom clock based on a diffractive optic,” *Opt. Express* **27**, 38359–38366 (Dec 2019).
- [24] Elgin, J. D., Heavner, T. P., Kitching, J., Donley, E. A., Denney, J., and Salim, E. A., “A cold-atom beam clock based on coherent population trapping,” *Applied Physics Letters* **115**(3), 033503 (2019).
- [25] Kim, S., Westly, D. A., Roxworthy, B. J., Li, Q., Yulaev, A., Srinivasan, K., and Aksyuk, V. A., “Photonic waveguide to free-space gaussian beam extreme mode converter,” *Light: Science & Applications* **7**(1), 72 (2018).
- [26] Chauhan, N., Bose, D., Puckett, M., Moreira, R., Nelson, K., and Blumenthal, D. J., “Photonic integrated Si_3N_4 ultra-large-area grating waveguide mot interface for 3d atomic clock laser cooling,” *Conference on Lasers and Electro-Optics*, STu4O.3, Optical Society of America (2019).

- [27] McGilligan, J. P., Griffin, P. F., Elvin, R., Ingleby, S. J., Riis, E., and Arnold, A. S., “Grating chips for quantum technologies,” *Scientific Reports* **7**, 384 (Mar. 2017).
- [28] Hunter, D., Jiménez-Martínez, R., Herbsommer, J., Ramaswamy, S., Li, W., and Riis, E., “Waveform reconstruction with a cs based free-induction-decay magnetometer,” *Opt. Express* **26**, 30523–30531 (Nov 2018).
- [29] Newman, Z. L., Maurice, V., Drake, T., Stone, J. R., Briles, T. C., Spencer, D. T., Fredrick, C., Li, Q., Westly, D., Ilic, B. R., Shen, B., Suh, M.-G., Yang, K. Y., Johnson, C., Johnson, D. M. S., Hollberg, L., Vahala, K. J., Srinivasan, K., Diddams, S. A., Kitching, J., Papp, S. B., and Hummon, M. T., “Architecture for the photonic integration of an optical atomic clock,” *Optica* **6**, 680–685 (May 2019).
- [30] Donley, E. A., Long, J. L., Liebisch, T. C., Hodby, E. R., Fisher, T. A., and Kitching, J., “Nuclear quadrupole resonances in compact vapor cells: The crossover between the nmr and the nuclear quadrupole resonance interaction regimes,” *Phys. Rev. A* **79**, 013420 (Jan 2009).
- [31] Affolderbach, C. and Mileti, G., “Tuneable, stabilised diode lasers for compact atomic frequency standards and precision wavelength references,” *Optics and Lasers in Engineering* **43**(3), 291–302 (2005). Optics in Switzerland.
- [32] Ye, J., Swartz, S., Jungner, P., and Hall, J. L., “Hyperfine structure and absolute frequency of the 87rb $5p3/2$ state,” *Opt. Lett.* **21**, 1280–1282 (Aug 1996).
- [33] Newman, Z. L., Maurice, V., Fredrick, C., Fortier, T., Leopardi, H., Hollberg, L., Diddams, S. A., Kitching, J., and Hummon, M. T., “High-performance, compact optical standard,” (2021).
- [34] Lee, K. I., Kim, J. A., Noh, H. R., and Jhe, W., “Single-beam atom trap in a pyramidal and conical hollow mirror,” *Opt. Lett.* **21**, 1177–1179 (Aug 1996).
- [35] Vangeleyn, M., Griffin, P. F., Riis, E., and Arnold, A. S., “Single-laser, one beam, tetrahedral magneto-optical trap,” *Opt. Express* **17**, 13601–13608 (Aug 2009).
- [36] Vangeleyn, M., Griffin, P. F., Riis, E., and Arnold, A. S., “Laser cooling with a single laser beam and a planar diffractor,” *Opt. Lett.* **35**, 3453–3455 (Oct 2010).
- [37] Nshii, C. C., Vangeleyn, M., Cotter, J. P., Griffin, P. F., Hinds, E. A., Ironside, C. N., See, P., Sinclair, A. G., Riis, E., and Arnold, A. S., “A surface-patterned chip as a strong source of ultracold atoms for quantum technologies,” *Nature Nanotechnology* **8**, 321–324 (Apr. 2013).
- [38] McGilligan, J. P., Griffin, P. F., Riis, E., and Arnold, A. S., “Phase-space properties of magneto-optical traps utilising micro-fabricated gratings,” *Opt. Express* **23**, 8948–8959 (Apr 2015).
- [39] “Kelvin nanotechnology grating magneto-optical trap.” <https://www.kntnano.com/quantum/gmotgrating/>.
- [40] McGilligan, J. P., Moore, K. R., Dellis, A., Martinez, G. D., de Clercq, E., Griffin, P. F., Arnold, A. S., Riis, E., Boudot, R., and Kitching, J., “Laser cooling in a chip-scale platform,” *Applied Physics Letters* **117**, 054001 (Aug. 2020).
- [41] Bregazzi, A., Griffin, P. F., Arnold, A. S., Burt, D. P., Martinez, G., Boudot, R., Kitching, J., Riis, E., and McGilligan, J. P., “A simple imaging solution for chip-scale laser cooling,” (2021).
- [42] McGehee, W. R., Zhu, W., Barker, D. S., Westly, D., Yulaev, A., Klimov, N., Agrawal, A., Eckel, S., Aksyuk, V., and McClelland, J. J., “Magneto-optical trapping using planar optics,” *New Journal of Physics* **23**, 013021 (jan 2021).
- [43] Bridge, E. M., Millen, J., Adams, C. S., and Jones, M. P. A., “A vapor cell based on dispensers for laser spectroscopy,” *Review of Scientific Instruments* **80**(1), 013101 (2009).
- [44] Kitching, J., Knappe, S., and Hollberg, L., “Miniature vapor-cell atomic-frequency references,” *Applied Physics Letters* **81**(3), 553–555 (2002).
- [45] Douahi, A., “Vapour microcell for chip scale atomic frequency standard,” *Electronics Letters* **43**, 279–280(1) (March 2007).
- [46] Henmi, H., Shoji, S., Shoji, Y., Yoshimi, K., and Esashi, M., “Vacuum packaging for microsensors by glass-silicon anodic bonding,” *Sensors and Actuators A: Physical* **43**(1), 243–248 (1994).
- [47] Hasegawa, M., Chutani, R., Gorecki, C., Boudot, R., Dziuban, P., Giordano, V., Clatot, S., and Mauri, L., “Microfabrication of cesium vapor cells with buffer gas for MEMS atomic clocks,” *Sensors and Actuators A: Physical* **167**, 594–601 (June 2011).

- [48] Stern, L., Bopp, D. G., Schima, S. A., Maurice, V. N., and Kitching, J. E., “Chip-scale atomic diffractive optical elements,” *Nature Communications* **10**(1), 3156 (2019).
- [49] Vicarini, R., Maurice, V., Abdel Hafiz, M., Rutkowski, J., Gorecki, C., Passilly, N., Ribetto, L., Gaff, V., Volant, V., Galliou, S., and Boudot, R., “Demonstration of the mass-producible feature of a cs vapor microcell technology for miniature atomic clocks,” *Sensors and Actuators A: Physical* **280**, 99–106 (2018).
- [50] Kohn, R. N., Bigelow, M. S., Spanjers, M., Stuhl, B. K., Kasch, B. L., Olson, S. E., Imhof, E. A., Hostutler, D. A., and Squires, M. B., “Clean, robust alkali sources by intercalation within highly oriented pyrolytic graphite,” *Review of Scientific Instruments* **91**(3), 035108 (2020).
- [51] Kang, S., Mott, R. P., Gilmore, K. A., Sorenson, L. D., Rakher, M. T., Donley, E. A., Kitching, J., and Roper, C. S., “A low-power reversible alkali atom source,” *Applied Physics Letters* **110**(24), 244101 (2017).
- [52] Kang, S., Moore, K. R., McGilligan, J. P., Mott, R., Mis, A., Roper, C., Donley, E. A., and Kitching, J., “Magneto-optic trap using a reversible, solid-state alkali-metal source,” *Optics Letters* **44**, 3002–3005 (Jun 2019).
- [53] McGilligan, J. P., Moore, K. R., Kang, S., Mott, R., Mis, A., Roper, C., Donley, E. A., and Kitching, J., “Dynamic characterization of an alkali-ion battery as a source for laser-cooled atoms,” *Phys. Rev. Applied* **13**, 044038 (Apr 2020).
- [54] Scherer, D. R., Fenner, D. B., and Hensley, J. M., “Characterization of alkali metal dispensers and non-evaporable getter pumps in ultrahigh vacuum systems for cold atomic sensors,” *Journal of Vacuum Science & Technology A* **30**(6), 061602 (2012).
- [55] Little, B. J., Hoth, G. W., Christensen, J., Walker, C., De Smet, D. J., Biedermann, G. W., Lee, J., and Schwindt, P. D. D., “A passively pumped vacuum package sustaining cold atoms for more than 200 days,” *AVS Quantum Science* **3**(3), 035001 (2021).
- [56] Burrow, O. S., Osborn, P. F., Boughton, E., Mirando, F., Burt, D. P., Griffin, P. F., Arnold, A. S., and Riis, E., “Centilitre-scale vacuum chamber for compact ultracold quantum technologies,” (2021).
- [57] Lee, J., Ding, R., Christensen, J., Rosenthal, R. R., Ison, A., Gillund, D. P., Bossert, D., Fuerschbach, K. H., Kindel, W., Finnegan, P. S., Wendt, J. R., Gehl, M., McGuinness, H., Walker, C. A., Lentine, A., Kemme, S. A., Biedermann, G., and Schwindt, P. D. D., “A cold-atom interferometer with microfabricated gratings and a single seed laser,” (2021).
- [58] Madkhaly, S., Coles, L., Morley, C., Colquhoun, C., Fromhold, T., Cooper, N., and Hackermüller, L., “Performance-optimized components for quantum technologies via additive manufacturing,” *PRX Quantum* **2**, 030326 (Aug 2021).
- [59] Cooper, N., Coles, L., Everton, S., Maskery, I., Campion, R., Madkhaly, S., Morley, C., O’Shea, J., Evans, W., Saint, R., Kruger, P., Orucevic, F., Tuck, C., Wildman, R., Fromhold, T., and Hackermüller, L., “Additively manufactured ultra-high vacuum chamber for portable quantum technologies,” *Additive Manufacturing* **40**, 101898 (2021).